DALTON
FULL PAPER

Multi-temperature X-ray diffraction, Mössbauer spectroscopy and magnetic susceptibility studies of a solvated mixed-valence trinuclear iron formate, $[Fe_3O(HCO_2)_6(NC_5H_4CH_3)_3]\cdot 1.3(NC_5H_4CH_3)$ †

Jacob Overgaard,[a] Eva Rentschler,[b] Grigore A. Timco,[c] Nicolae V. Gerbeleu,[c] Vladimir Arion,[d] Azzedine Bousseksou,[d] Jean Pierre Tuchagues[d] and Finn K. Larsen*[a]

[a] *Department of Chemistry, University of Aarhus, Langelandsgade 140, DK-8000 Aarhus C, Denmark. E-mail: kre@chem.au.dk*
[b] *MPI für Strahlenchemie, D-45470 Muelheim, Germany*
[c] *Institute of Chemistry, Academy of Sciences of the Republic of Moldova, Academiei Str. 3, MD-2028 Chisinau, Moldova*
[d] *Laboratoire de Chimie de Coordination, UPR CNRS 8241, 205 route de Narbonne, F-31077 Toulouse Cedex 04, France*

Received 21st March 2002, Accepted 27th May 2002
First published as an Advance Article on the web 5th July 2002

Structural analysis of the solvated mixed-valence (MV) trinuclear iron carboxylate, $[Fe_3O(HCO_2)_6(\gamma\text{-pic})_3]\cdot x(\gamma\text{-pic})$, **1**, (γ-pic = 4-methylpyridine; $x \approx 1.3$), has been performed from X-ray diffraction data at four temperatures. Analysis of the X-ray diffraction and variable temperature Mössbauer data for **1** clearly shows the presence of localised valence states for iron atoms at and below 100 K. Both physical methods agree that compound **1** exhibits a continuously growing degree of electron transfer (ET) between the three iron sites with increasing temperature; however, the extent of ET is significantly larger for one of the iron(III) sites. All three terminal γ-pic groups remain ordered at and below room temperature, whereas the γ-pic solvent molecules have a temperature dependent disorder over a number of positions. The distribution of the solvent over disorder positions is suggested to influence the degree of ET between the metal sites. From the molecular geometry in the Fe_3O-core, an estimate of 260 cm^{-1} in energy difference between the two vibronic states corresponding to electronic localisation on either of the two iron atoms involved in ET is obtained. This value is close to an estimate for the energy difference assessed by using a Blume–Emery–Griffith Hamiltonian to describe the localised–delocalised transition in mixed valence molecular compounds.

Introduction

It has long been known that many compounds belonging to the mixed-valence class of basic iron carboxylates with the general molecular formula, $[Fe_2^{III}Fe^{II}(\mu^3\text{-}O)(RCO_2)_6L_3]\cdot S$ (S = solvent), can exhibit temperature dependent electron transfer (ET) between the three iron sites.[1] More recently, it has been discovered that in some of these complexes, the ET apparently involves only two of the three iron sites, leaving the third in a trivalent oxidation state in the entire temperature regime.[2] The temperature dependence of the ET varies considerably from compound to compound; it is for instance found that the changes from a localised valence state to a completely delocalised state can be abrupt and have the characteristics of a phase transition[3] or take place slowly over an extended temperature range.[4] Several characteristic structural features, such as changes in solvent or ligand disorder and intermolecular hydrogen bonding patterns between solvent and molecule,[2] have been introduced as explanations for phase transitions and the temperature dependence of the ET. These studies have indicated clearly that changes in the thermal motion of either solvent or ligands may be strongly correlated to changes in the ET between the metal atoms. Nevertheless, structural studies at several temperatures covering both sides of the valence trapping temperature have only been performed for a few compounds, despite the wealth of information made accessible from such experiments. Instead, information on the temperature dependence of the ET has in many cases been extracted from Mössbauer spectroscopic studies of the systems, in combination with a structural investigation at only one temperature. So far a relatively large number of mixed valence trinuclear oxo-bridged iron aliphatic, aromatic and halogen-containing carboxylates have been obtained. However, no such compounds have been documented yet for formic acid. The formate is the simplest member of the broad range of mixed-valence iron carboxylates and avoids the problems related to the frequently encountered disorder of the carboxylic substituents (R). In this paper we report the structural results of a diffraction study of the mixed-valence compound $[Fe_2^{III}Fe^{II}O(HCO_2)_6(\gamma\text{-pic})_3]\cdot 1.3(\gamma\text{-pic})$, **1**, Fig. 1, at a number of temperatures above and below the onset temperature of ET. Furthermore, results of variable temperature Mössbauer studies and magnetic susceptibility measurements of **1** are also given.

Experimental

Synthesis

One of the main procedures — besides ligand exchange — that was used for obtaining the trinuclear mixed-valence compounds of the type $[Fe^{III}_2Fe^{II}O(O_2CR)_6L_3]\cdot xS$, was controlled oxidation of iron(II) carboxylates. The procedure is based on the fact that the oxidising process of iron(II) carboxylates until their complete oxidation into iron(III) carboxylates proceeds in

† Electronic supplementary information (ESI) available: temperature dependence of the Fe–O_e and Fe–N bond distances. See http://www.rsc.org/suppdata/dt/b2/b202851d/

Table 1 Crystallographic details for **1**

	100 K	180 K	240 K	295 K
Space group	*C*2/*c*	*C*2/*c*	*C*2/*c*	*C*2/*c*
λ/Å	0.7107	0.7107	0.7107	0.7107
a/Å	24.303(3)	24.382(3)	24.466(2)	24.495(5)
b/Å	27.360(3)	27.485(4)	27.516(3)	27.532(6)
c/Å	12.433(1)	12.513(2)	12.602(1)	12.685(3)
β/°	96.645(3)	96.562(4)	96.440(3)	96.221(9)
V/Å^3	8212(3)	8330(3)	8430(2)	8505(3)
Z	8	8	8	8
μ/mm^{-1}	1.11	1.11	1.11	1.11
T/K	100	180	240	295
R_{int}	0.024	0.068	0.072	0.043
$R(F)$, no. of reflections	0.058, 7210	0.081, 8020	0.095, 6429	0.077, 5205
$R_w(F^2)$, number of reflections	0.188, 10794	0.253, 15384	0.293, 15509	0.277, 9988
No. of parameters	454	454	454	454

$R(F) = \Sigma(F_{obs} - F_{calc})/\Sigma F_{obs}$; $R(F^2) = \Sigma(F_{obs}^2 - F_{calc}^2)^2/\Sigma F_{obs}^2$, $S = \{\Sigma w_i(F_{obs}^2 - F_{calc}^2)/\Sigma(n-p)\}^{1/2}$.

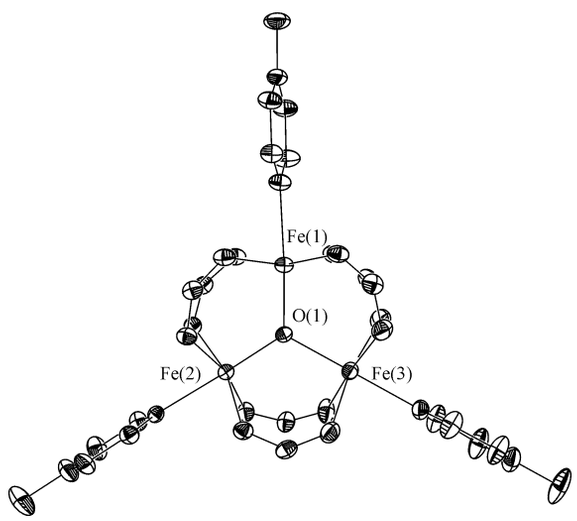

Fig. 1 An ORTEP[17] view of the $Fe_3O(HCO_2)_6(\gamma\text{-pic})_3$ molecular entity at 100 K. Thermal ellipsoids correspond to 50% probability.

steps, with the formation of clusters of iron atoms in oxidation state +2 and +3 in different ratios. The formation and isolation of mixed valence iron compounds using this procedure is facilitated by their different solubility compared to that of the initial iron(II) and iron(III) carboxylates. This methodology was the first, largely used by Gerbeleu *et al.*,[5] for synthesising complexes with a $Fe_2^{III}Fe^{II}O$ core with other aliphatic carboxylic acids besides the acetate anion. It has since proven to be quite effective for obtaining mixed-valence iron formates.

Compound A: $[Fe_4(HCO_2)_{10}(\gamma\text{-pic})_6]_n$. A mixture of powdered metallic iron (1.0 g), formic acid (10 mL), water (3 mL) and γ-picoline (25 mL) was refluxed in air at 100 °C with stirring for 5 hours. The resultant solution, which had changed colour from yellow to green, was filtered hot through a fine filter paper in air and the flask was closed with a cork. After a week the obtained crystalline product was separated by filtration under an argon atmosphere, washed thoroughly with γ-picoline and acetone and dried in an argon flow. The product consisted of small, blue-coloured, square-plate-shaped crystals and was isolated in 4.2 g (76%) yield. (Found: C, 44.69; H, 4.22; N, 6.76; Fe, 18.40. $C_{23}H_{26}Fe_2N_3O_{10}$ requires C, 44.83; H, 4.25; N, 6.82; Fe, 18.13%). The structure of compound **A** is reported elsewhere.[6]

Compound 1: $[Fe_3O(HCO_2)_6(\gamma\text{-pic})_3]\cdot 1.3(\gamma\text{-pic})$. Compound **A** (2.5 g) was dissolved in boiling γ-picoline (25 mL) by heating and stirring the mixture in air for 15 min. The black solution obtained was filtered hot through a fine filter paper and cooled slowly in an inert atmosphere. After 12 h large black–brown crystals were isolated by filtration and washed with cold γ-picoline and pentane and dried in an inert atmosphere. The compound was sensitive to air. Yield 1.35 g (58%). (Found: C, 44.52; H, 4.29; N, 7.09; Fe, total 19.81; Fe^{II}, 6.48. $C_{31.8}H_{36.1}Fe_3N_{4.3}O_{13}$ requires C, 44.72; H, 4.26; N, 7.05; Fe, total 19.62; Fe^{II}, 6.54%).

Single crystal X-ray diffraction

Black crystals of compound **1** (data collection temperature, size: 100 and 295 K, 0.50 × 0.35 × 0.12 mm^3; 180 and 240 K, 0.50 × 0.31 × 0.18 mm^3) were mounted in oil on the tip of a few carbon fibre strands attached to a thin copper wire which was soldered to a brass pin. This assembly was placed on the goniometer head of a Bruker SMART 1000 CCD diffractometer at the Department of Chemistry at the University of Aarhus. The sample crystal was cooled using an Oxford Cryosystems device and a complete hemisphere of data was collected using Mo-Kα-radiation (λ = 0.71073 Å). Further crystal data and data collection information are given in Table 1. The data were integrated and subsequently empirically absorption corrected using the SAINT+ program package.[7]

The structure at 100 K was solved with direct methods using SHELXTL,[8] which immediately gave all non-H atoms in the trinuclear complex. Hydrogen atoms were placed at calculated positions and refined as riding atoms in the subsequent least squares model refinement. Their isotropic thermal parameter was estimated to be 1.2 times the value of the equivalent isotropic thermal parameter of the atom to which hydrogen is bonded. All non-H atoms in the trinuclear molecule were refined with anisotropic thermal parameters. Several groups of peaks appeared in a difference Fourier map at some distance from the main molecule. Three of such groups were identified as γ-picoline, and they were subsequently refined with constraints that forced the groups to resemble the γ-picoline ligands in the trinuclear molecule. The solvent molecules were given occupation factors which were refined and, for the models at 240 and 295 K, atoms in each solvent group were assigned a common thermal parameter, except for the atoms of the methyl groups which were put at a value 20% higher than the rest of the molecule. Crystallographic details for each temperature are summarised in Table 1.

CCDC reference numbers 173994–173997.

See http://www.rsc.org/suppdata/dt/b2/b202851d/ for crystallographic data in CIF or other electronic format.

Mössbauer spectroscopy measurements

Mössbauer spectra were recorded on a constant acceleration conventional spectrometer with a 50 mCi source of ^{57}Co (Rh matrix). Isomer shift values (δ) are quoted relative to room-temperature α-iron foil. The absorber was a sample of 100 mg of microcrystalline powder enclosed in a 20 mm

Table 2 Selected average bond lengths (Å) in **1**

	100 K	180 K	240 K	295 K
Fe(1)–O(1)	1.856(3)	1.872(2)	1.882(3)	1.891(4)
Fe(2)–O(1)	1.847(2)	1.853(3)	1.855(3)	1.854(1)
Fe(3)–O(1)	2.023(3)	2.017(3)	2.003(3)	1.984(4)
Δd_{obs} [a]	0.167	0.145	0.121	0.093
⟨Fe(1)–O_e⟩	2.04(2)	2.05(2)	2.05(1)	2.06(2)
⟨Fe(2)–O_e⟩	2.03(2)	2.04(2)	2.04(2)	2.04(1)
⟨Fe(3)–O_e⟩	2.13(1)	2.13(1)	2.12(1)	2.10(2)
Fe(1)–N	2.206(3)	2.212(3)	2.219(4)	2.227(5)
Fe(2)–N	2.195(3)	2.208(3)	2.213(4)	2.212(5)
Fe(3)–N	2.166(3)	2.180(4)	2.181(5)	2.189(5)
⟨C–O_e⟩ bound to Fe(3)	1.231(5)	1.234(9)	1.232(11)	1.227(13)
⟨C–O_e⟩ bound to Fe(1,2) [b]	1.256(3)	1.254(3)	1.254(2)	1.243(6)

[a] $\Delta d_{obs} \equiv (d(Fe(3)–O(1)) - d(Fe(1)–O(1)))$. [b] Average C–O distance for the oxygens bound to either Fe(1) or Fe(2) in formate groups bridging Fe(3) with Fe(1) or Fe(2).

diameter plastic sample holder, the size of which had been determined to optimise the absorption. Variable temperature spectra were obtained in the 80–330 K range, using a MD306 Oxford cryostat, the thermal scanning being monitored by an Oxford ITC4 servocontrol device (±0.1 K accuracy). A least-squares computer program[9] was used to fit the Mössbauer parameters and determine their standard deviations (given in parentheses).

Magnetic susceptibility measurements

Temperature dependent magnetic susceptibility measurements were performed in a Quantum Design SQUID-Magnetometer MPMS in the temperature range of 2 to 298 K in an applied magnetic field of 1 T. The experimental data were corrected for the diamagnetic contribution using Pascal's constants.

Results and discussion

Synthesis

The synthesis of compound **1** has been performed in good yield by a two step procedure. The reaction of powdered iron with an excess of formic acid and γ-picoline in the presence of a small amount of water produced the mixed-valence polymeric complex $[Fe^{III}_2Fe^{II}_2(HCO_2)_{10}(\gamma\text{-pic})_6]_n$ with an interesting layer structure.[6] Subsequent oxidation of this complex in γ-picoline by heating it in air for a short time resulted in the trinuclear product $[Fe^{III}_2Fe^{II}O(HCO_2)_6(\gamma\text{-pic})_3]\cdot 1.3(\gamma\text{-pic})$.

Structural analysis

The molecule of the title compound contains a planar $Fe_3(\mu_3\text{-}O)$-core. Six formate groups bridge the iron atoms and three γ-pic molecules fulfil the octahedral coordination of each iron, Fig. 1. Disordered γ-pic molecules occupy half of the inter-molecular cavities in the structure.

The temperature dependence of the ET taking place between iron sites in the trinuclear iron complexes can be elucidated by the changes in Fe–O(1) and Fe–ligand bond distances as a function of temperature.[4] Values for complex **1** are listed in Table 2, and Fig. 2 illustrates the temperature dependence of Fe–O(1) bond distances which are the most sensitive to changes in the average oxidation state of the individual iron atoms. Fe(2)–O(1) remains practically unaffected by temperature but the Fe(1)–O(1) and Fe(3)–O(1) distances change significantly. Even at room temperature the compound is partly valence trapped. As the temperature is lowered Fe(1)–O(1) converges towards 1.85 Å, the same bond length as that of Fe(2)–O(1), which is indicative of a valence ordered Fe^{III} atom. Fe(3)–O(1) converges towards 2.03 Å, typical of Fe^{II}. The influence on the iron–formate (Fe–O_e) and Fe–N bonds of increasing valence disorder is less, but still significant (see ESI). The trends in the

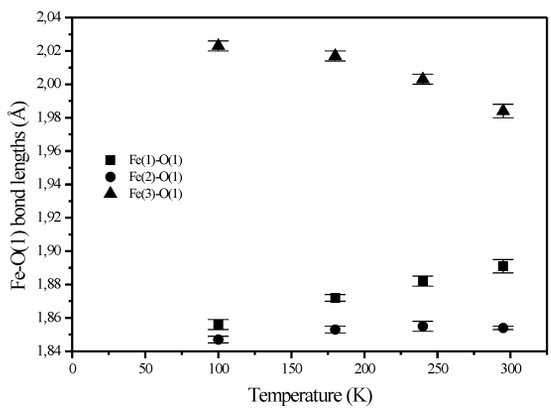

Fig. 2 Fe–O(1) bond distances in the central region of **1**. The bars above and below the bond values indicate ±1 esd.

Fe–O_e bond distances show similar behaviour to the Fe–O(1) bonds. As in other trinuclear complexes, a *trans*-effect, which lengthens the Fe–N bond *trans* to the Fe–O(1) bond and *vice versa*, is observed.[3] The longest distance, Fe(3)–O(1) as expected corresponds to the shortest Fe–N distance and Fe(3)–N expectedly decreases as Fe(3)–O(1) increases. In conclusion, the Fe-ligand geometries suggest that ET takes place predominantly between two of the three Fe sites, a behaviour which until now has only been observed in a few other compounds.[2]

The packing pattern of the trinuclear molecules is shown in Fig. 3. In the crystal the Fe_3O-planes of the trinuclear molecules are arranged in layers parallel to the (101) crystal planes. In the perpendicular view of the layers, Fig. 3, it can be seen that

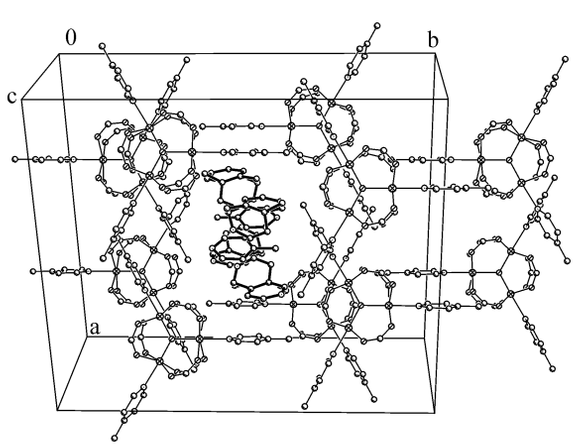

Fig. 3 Packing diagram viewed perpendicular to the Fe_3O planes. Two types of void, one partly occupied and one apparently empty, can be seen between the trinuclear iron carboxylate molecules.

the shortest intermolecular interaction is between the γ-picoline ligands, bonded to Fe(1) and Fe(2). The planes form an angle of 11.5° and are separated by a distance of 3.7 Å. The γ-picoline ligand planes are all close to perpendicular to the central Fe_3O-plane, forming angles in the range from 87.9 to 99.4° (see also Fig. 1). The trinuclear molecules pack to form two different voids. In one of them, γ-picoline solvent molecules were found at three partly occupied positions. The traces of solvent in the other cavity, located by difference Fourier, were so insignificant at 100 K that they were not included in the model.

The occupation of the different solvent molecular positions also show interesting temperature dependencies (Fig. 4). A

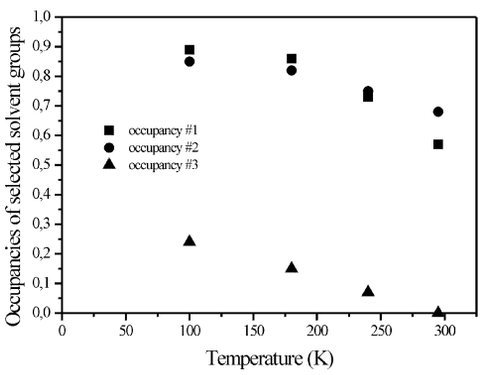

Fig. 4 Solvent disorder as a function of temperature for the three different disorder positions.

continuous decrease in occupation is observed for increasing temperature. It should be noted that two different crystals were used for collecting the four data sets in the temperature order 100, 295, 240 and 180 K. One crystal was used for the first two temperatures and another for the remaining two sets. The observation shown in Fig. 4 therefore is hardly due to volatilisation of solvent molecules with increasing temperature. We interpret it as being due to increasing disorder, *i.e.* solvent molecules being redistributed to populate other orientations and positions than included in the low-temperature model. The highest peaks in the difference Fouriers are found in the voids of the structure indicating that solvent molecules tend to order in one void at the lowest temperature and increasingly diffuse to occupy both voids in the structure at higher temperatures. Such an order–disorder transition of the solvent has previously been shown to affect the degree of ET in related trinuclear complexes.[10]

Potential energy surface in 1

The temperature dependence of the bond lengths in the central molecular region reveals details of the ability of the "extra" electron to travel between different iron sites. Assuming that the potential energy surface is constant in the temperature interval 100–295 K, the relative distribution of the extra electron on the two iron sites most involved in the ET process can be approximated to be of Boltzmann-type: $(P_I/P_{II}) = \exp(-\Delta E/kT)$, with a constant energy difference of ΔE. P denotes the population of (I) the higher lying and (II) the lower lying vibronic states. At a certain temperature, the difference in bond lengths (Δd_{obs}) between the two Fe–O(1) bonds involved in ET and the similar difference in the valence trapped state (Δd_{trap} = 0.176 Å) can be correlated to the relative populations of the vibronic levels: $(P_I/P_{II}) = (\Delta d_{trap} - \Delta d_{obs})/(\Delta d_{trap} + \Delta d_{obs}) = \exp(-\Delta E/kT)$. Thus, plotting ln $((\Delta d_{trap} + \Delta d_{obs})/(\Delta d_{trap} - \Delta d_{obs}))$ as a function of $(1/T)$ will give the energy difference between vibronic levels. This is shown in Fig. 5. A linear regression line including also the zero-point as an observation has a good fit of R = 0.988 with a slope corresponding to a value ΔE = 260 cm^{-1}. This value is between those found for two

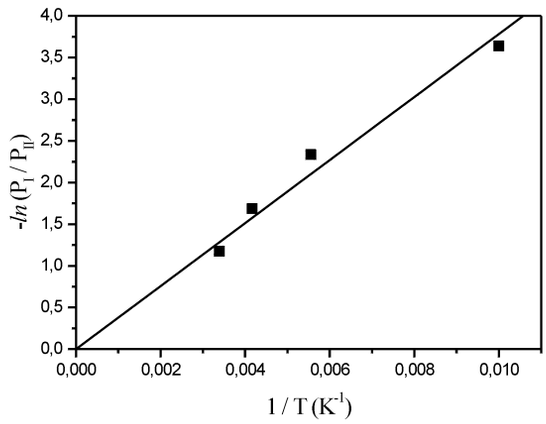

Fig. 5 Energy barrier diagram showing $-\ln(P_I/P_{II}) = \Delta E/kT$. ΔE is calculated from the slope (a) of the least-squares fitted line as: $a = \Delta E/k$. $\Delta E = a \times 1.380 \times 10^{-23} \times 5.034 \times 10^{22} = a \times 0.695$ cm^{-1}.

other trinuclear iron carboxylates in a similar manner (for $[Fe_3O(O_2CC(CH_3)_3)_6(NC_5H_5)_3]$ ΔE = 44 cm^{-1} (ref. 4) and for $[Fe_3O(O_2CCH_3)_6(3\text{-Cl-py})_3]\cdot 3\text{-Cl-py}$ ΔE = 410 cm^{-1} (ref. 3*b*)).

Mössbauer spectroscopy

Representative Mössbauer spectra of compound **1** recorded in the warming mode are shown in Fig. 6 and values of the

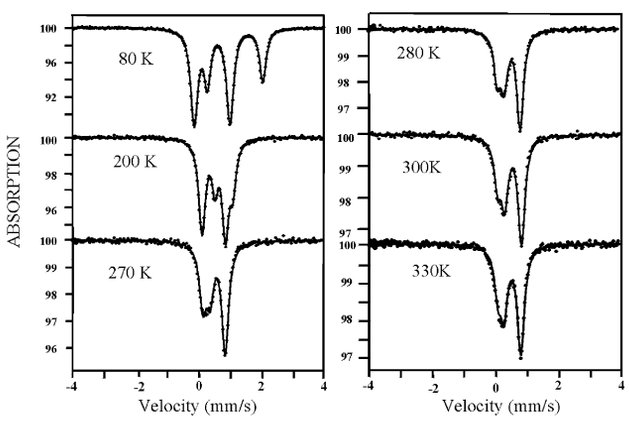

Fig. 6 Representative Mössbauer spectra of $[Fe_3O(HCO_2)_6(\gamma\text{-pic})_3]\cdot 1.3(\gamma\text{-pic})$, **1**, obtained in the warming mode.

Mössbauer parameters obtained by least-squares fitting of the spectra are gathered in Table 3. At 80 K, the Mössbauer spectrum consists of three quadrupole-split doublets, with isomer shift values δ = 0.538, 0.544 and 1.240 mm s^{-1} and quadrupole splittings ΔE_Q = 1.172, 1.008 and 1.686 mm s^{-1} typical of high-spin iron(III) (first two values) and high-spin iron(II), respectively. Mössbauer spectra show unbroadened quadrupole split doublets in the whole 80–330 K temperature range, allowing their unambiguous fitting with respect to the criterion of continuity in thermal variation of δ and ΔE_Q (Figs. 7a and 7b, respectively). The unusually large variation in δ of the "Fe^{II}" site (1.240–0.69 mm s^{-1}) can not be attributed to the classical 2nd order Doppler effect law.[11] Above ~240 K the spectra do not simply allow identification of Fe^{II} and Fe^{III} signals: as temperature is increased, (i) the three doublets get closer to each other, and (ii) the decrease in δ of the "Fe^{II}" site (1.240–0.69 mm s^{-1}) is much larger than the increase in δ of the Fe^{III} sites (0.538–0.626 and 0.544–0.67 mm s^{-1}). This is what would be expected from an averaging process occurring rapidly relative to the Mössbauer time scale. The absence of significant broadenings also indicates that the temperature dependent ET between iron sites, evidenced by the changes in Fe–O(1) and Fe–ligand bond distances in compound **1**, is much faster than the Mössbauer time scale (10^7–10^8 s^{-1}).[12] The large decrease in

Table 3 Representative least-squares-fitted Mössbauer data for compound **1**

	Fe(2)			Fe(1)			Fe(3)		
T/K	δ	ΔE_Q	$\Gamma/2$	δ	ΔE_Q	$\Gamma/2$	δ	ΔE_Q	$\Gamma/2$
80	0.538(1)	1.172(3)	0.116(1)	0.544(1)	1.008(3)	0.116(1)	1.240(1)	1.686(2)	0.116(1)
120	0.553(1)	1.049(2)	0.114(1)	0.556(1)	0.919(2)	0.114(1)	1.167(1)	1.346(1)	0.114(1)
160	0.558(3)	0.838(4)	0.113(2)	0.614(3)	0.831(4)	0.113(2)	1.049(2)	0.904(3)	0.113(2)
200	0.604(2)	0.779(6)	0.111(2)	0.626(2)	0.667(6)	0.111(2)	0.928(2)	0.554(3)	0.111(2)
220	0.606(3)	0.746(7)	0.113(2)	0.636(3)	0.629(8)	0.113(2)	0.874(2)	0.465(3)	0.113(2)
240	0.611(3)	0.749(5)	0.110(2)	0.643(3)	0.581(6)	0.110(2)	0.826(3)	0.437(4)	0.110(2)
260	0.626(3)	0.786(6)	0.113(2)	0.661(6)	0.60(2)	0.113(2)	0.750(6)	0.38(1)	0.113(2)
270	0.619(5)	0.77(1)	0.118(3)	0.66(5)	0.58(9)	0.118(3)	0.74(5)	0.42(9)	0.118(3)
280	0.61(2)	0.76(3)	0.116(3)	0.67(2)	0.59(4)	0.116(3)	0.721(7)	0.42(2)	0.116(3)
300	0.59(5)	0.77(9)	0.120(3)	0.67(4)	0.60(9)	0.120(3)	0.699(8)	0.45(2)	0.120(3)
310	0.59(4)	0.77(8)	0.125(3)	0.67(4)	0.61(8)	0.125(3)	0.686(6)	0.46(2)	0.125(3)
330	0.56(6)	0.8(1)	0.135(7)	0.64(7)	0.6(1)	0.135(7)	0.69(6)	0.5(1)	0.135(7)

Isomer shifts (δ, mm s^{-1}) refer to metallic iron at room temperature; ΔE_Q = quadrupole splitting (mm s^{-1}); $\Gamma/2$ = half-width of the lines (mm s^{-1}); statistical standard deviations are given in parentheses. In order for each site to account for 1/3 of the total absorption, the numbers of counts and the half-width of the lines have been considered equal for all three sites.

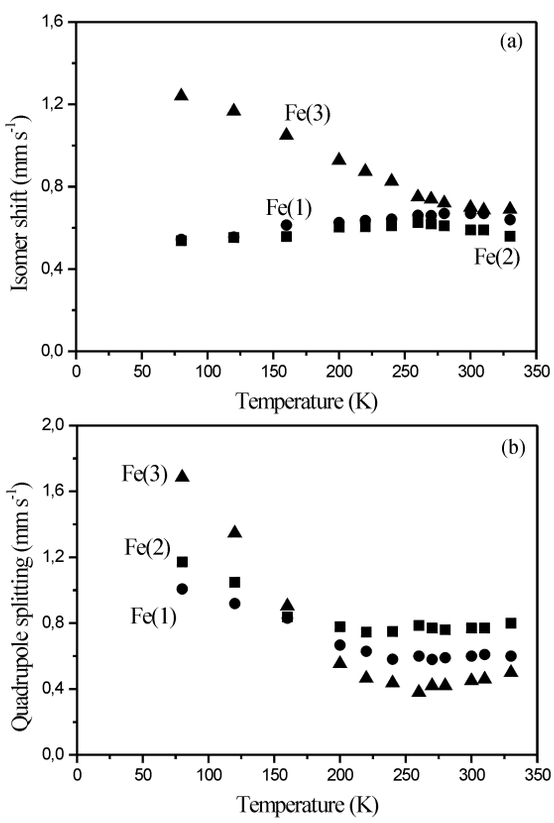

Fig. 7 Temperature dependence of (a) the isomer shift and (b) the quadrupole splittings for the iron sites of $[Fe_3O(HCO_2)_6(\gamma\text{-pic})_3]\cdot 1.3(\gamma\text{-pic})$, **1**.

δ of the "Fe^{II}" site associated to the small increase in δ of the "Fe^{III}" sites with increasing temperature evidences an increased ferric character of the "Fe^{II}" site when temperature is increased from 100 to 330 K. However, complete delocalisation is not reached as confirmed by the X-ray structural data.

The "fusion type" temperature dependence of Mössbauer spectra[12] for compound **1** (quadrupole split doublets of Fe^{II} and Fe^{III} getting very close to each other without significant line broadening) is similar to that previously reported for a few closely related trinuclear iron carboxylates.[2c,3a,13] However, significant differences in the spectral characteristics of these $[Fe_2^{III}Fe^{II}(\mu_3\text{-O})(RCO_2)_6L_3]\cdot S$ compounds deserve to be mentioned. In $[Fe_2^{III}Fe^{II}(\mu_3\text{-O})(CH_2ClCO_2)_6(H_2O)_3]\cdot 3H_2O$,[2c] the three iron sites are distinguished by Mössbauer spectroscopy and ET only takes place between two of the three iron atoms over a rather large temperature range (T ~ 100–300 K) without crystallographic phase transition. In $[Fe_2^{III}Fe^{II}(\mu_3\text{-O})(CH_2CNCO_2)_6(H_2O)_3]$,[3a] only two iron sites (Fe^{II} and Fe_2^{III}) are distinguished by Mössbauer spectroscopy and ET takes place between the three iron atoms over a narrow temperature range around T = 130 K with crystallographic phase transition. In $[Fe_2^{III}Fe^{II}(\mu_3\text{-O})(CH_3CO_2)_6(4\text{-Etpy})_3]\cdot(4\text{-Etpy})$,[13] only two iron sites (Fe^{II} and Fe_2^{III}) are distinguished by Mössbauer spectroscopy and ET takes place between the three iron atoms over a rather large temperature range (T ~ 100–300 K) without crystallographic phase transition. In compound **1**, the situation is intermediary between those described for $[Fe_2^{III}Fe^{II}(\mu_3\text{-O})(CH_2ClCO_2)_6(H_2O)_3]\cdot 3H_2O$,[2c] and $[Fe_2^{III}Fe^{II}(\mu_3\text{-O})(CH_3CO_2)_6(4\text{-Etpy})_3]\cdot(4\text{-Etpy})$:[13] while three iron sites are distinguished by Mössbauer spectroscopy, ET takes predominantly place between two of the three iron atoms over a rather large temperature range (T ~ 100–300 K) without crystallographic phase transition.

As suggested by Hendrickson *et al.*[13] the "fusion type" temperature dependence observed in the Mössbauer spectra of a few mixed valence trinuclear iron carboxylates is not just the result of thermally activating complex molecules to overcome the potential-energy barrier for ET: the observed temperature dependencies are most likely the manifestation of thermal motion of ligand and/or solvate molecules in the solid, not directly intramolecular ET. In agreement with the decrease in occupation of the different solvent molecular positions of **1** on increasing temperature (Fig. 4), the "fusion type" temperature dependence of the Mössbauer spectra is probably the result of an order–disorder phase transition. The phonon mode activating the order–disorder phase transition is obviously occurring at a frequency much higher than the Mössbauer time scale, thus preventing the line broadenings usually associated to the averaging process.

The energy difference ΔE between the vibronic levels corresponding to the two iron sites among which the extra electron is distributed may be assessed by using a Blume–Emery–Griffith Hamiltonian to describe the localised–delocalised (LD) transition in mixed valence molecular compounds as previously suggested.[11] In this model, three electronic levels have been introduced through a fictitious spin S_z = 0, ±1. As a rough approximation, we may only consider the S_z = ±1 levels. By comparison with thermodynamic or Ising-like models for spin-crossover compounds,[14] one can write: $\Delta E = T_{equ}\Delta S$ and $\Delta S = R$ ln (ge/gf) where T_{equ} is the equilibrium temperature of the system (~280 K in the present case), ΔS is the entropy variation upon the LD transition, R = 8.314 J K^{-1}mol^{-1}, and ge/gf is the degeneracy ratio of the +1 and −1 levels. ge/gf includes terms of electronic and vibrational origin:[14] $ge/gf = (ge/gf)^{el} \times$

$(ge/gf)^{vib}$ and $(ge/gf)^{el} = (2S + 1)^{excited}/(2S + 1)^{ground} = 6/5$. The crystallographic data mentioned above show that the variation in metal–ligand distance upon LD transition in compound **1** is ~18% of the corresponding variation (~0.2 Å) in spin-crossover complexes where $(ge/gf)^{vib}$ ~80–200. One can thus state that in the present case $(ge/gf)^{vib}$ ~ 14–36, leading to ge/gf ~ 17–43 and ΔE ~ 6.6–8.8 kJ mol^{-1}. The ΔE value estimated in the Potential energy surface section above (260 cm^{-1}, 3.1 kJ mol^{-1}) is rather close to the ΔE range resulting from this rough approximation. It is finally remarkable to note that the ΔE energy difference between the two vibronic states of 1′,1″-diethylbiferrocenium triiodide, also showing fusion type averaging process of its mixed-valence state, is in the same range (750 cm^{-1}, 9 kJ mol^{-1}).[15]

Magnetic susceptibility

Fig. 8 shows the variable temperature molar magnetic susceptibility of **1**. The overall temperature dependence of the χT product clearly indicates antiferromagnetic interaction. With decreasing temperature the value for χT decreases slowly from 3.3 emu K mol^{-1} at room temperature to a plateau of 2.2 emu K mol^{-1} at around 50 K. Further lowering of the temperature finally leads to a sharp decrease of χT leading to 1.0 emu K mol^{-1} at 2 K. The experimental data could be simulated perfectly applying a two-J model to the HDvV-Hamiltonian:

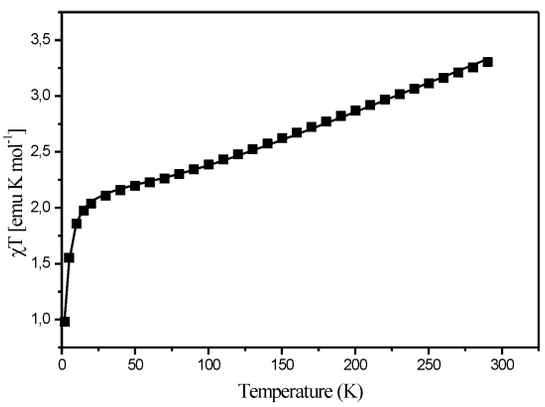

Fig. 8 Variable-temperature magnetic susceptibility measurements of **1**.

$$H = -2J_{ab}(S_a \cdot S_b) - 2J(S_a \cdot S_c + S_b \cdot S_c)$$

with S_a and S_b being the Fe(III) sites with spins equal to 5/2 and S_c being the Fe(II) site with a spin of 2.

Least squares refinements lead to the two different exchange interactions, $J_{ab} = -62.9$ cm^{-1} and $J = -21.8$ cm^{-1}, between Fe(III)–Fe(III) and Fe(III)–Fe(II), respectively. The ratio 3/1 for J_{ab}/J is in good agreement with other reported ratios for the exchange coupling constants in mixed-valent oxo-centred trinuclear iron complexes.[16] The calculated energy ladder shows only a very small energy gap of 5 cm^{-1} between the spin ground state $(S,S_{ab}) = (1,1)$ and the first excited state (2,0). The energy separation to the next excited states of (2,1) and (0,2) however are found to be much larger with 87 and 121 cm^{-1}, respectively, thus allowing modelling of the magnetisation data for the iron sites with localised valences, while the X-ray study and Mössbauer data clearly show ET as a function of temperature.

Conclusions

Multi-temperature structural studies show the presence of an onset temperature in the vicinity of 100 K for electron transfer in the solid state of the trinuclear complex. The structural analysis leads to an estimate of the energy difference between adjacent vibronic levels. This value is close to an estimate for the energy difference assessed by using a Blume–Emery–Griffith Hamiltonian to describe the LD transition in mixed valence molecular compounds. The change in the occupancy with temperature of γ-picoline solvent molecules can be correlated to the gradual change in ET as a function of temperature.

Analysis of variable temperature Mössbauer data for **1** confirms the presence of localised valence states for iron atoms at 80 K and a continuously growing degree of ET between the three iron sites on increasing temperature. However, complete delocalisation is not reached as confirmed by the X-ray structural data and the extent of ET is significantly larger for one of the iron(III) sites. The "fusion type" temperature dependence observed in the Mössbauer spectra is most likely the result of an order–disorder phase transition of solvate molecules in the solid, activated by a phonon mode occurring at a frequency much higher than the Mössbauer time scale, thus preventing the line broadenings usually associated to the averaging process.

References

1 D. N. Hendrickson, in *Mixed Valency Systems: Applications in Chemistry, Physics and Biology*, ed. K. Prassides, Kluwer Academic Publishers, Dordrecht, 1991, pp. 67–90; R. D. Cannon and R. P. White, *Prog. Inorg. Chem.*, 1988, **36**, 195.

2 (*a*) M. Manago, S. Hayami, Y. Yano, K. Inoue, R. Nakata, A. Ishida and Y. Maeda, *Bull. Chem. Soc. Jpn.*, 1999, **72**, 2229; (*b*) R. Wu, M. Poyraz, F. E. Sowrey, C. E. Anson, S. Wocadlo, A. K. Powell, U. A. Jayasooriya, R. D. Cannon, T. Nakamoto, M. Katada and H. Sano, *Inorg. Chem.*, 1998, **37**, 1913; (*c*) T. Sato, F. Ambe, K. Endo, M. Katada, H. Maeda, T. Nakamoto and H. Sano, *J. Am. Chem. Soc.*, 1996, **118**, 3450.

3 (*a*) T. Nakamoto, M. Hanaya, M. Katada, K. Endo, S. Kitagawa and H. Sano, *Inorg. Chem.*, 1997, **36**, 4347; (*b*) C.-C. Wu, S. A. Hunt, P. K. Gantzel, P. Güttlich and D. N. Hendrickson, *Inorg. Chem.*, 1997, **36**, 4717; (*c*) K. Asamaki, T. Nakamoto, S. Kawata, H. Sano, M. Katada and K. Endo, *Inorg. Chim. Acta*, 1995, **236**, 155.

4 C. Wilson, B. B. Iversen, J. Overgaard, F. K. Larsen, G. Wu, S. P. Palii, G. A. Timco and N. V. Gerbeleu, *J. Am. Chem. Soc.*, 2000, **122**, 11370; M. L. Hansen, Masters Thesis, University of Aarhus, 2000.

5 N. V. Gerbeleu, G. A. Timco, K. I. Turta, G. A. Popovich, S. A. Bobkova and K. M. Indrichan, *Russ. J. Inorg. Chem.*, 1986, **31**, 390.

6 J. Overgaard, Ph. D. Thesis, University of Aarhus, 2001.

7 SAINT+, v6.02, Bruker AXS, Madison, WI, USA, 1999.

8 SHELXTL, v5.01, Bruker AXS, Madison, WI, USA, 1998.

9 F. Varret, *Proceedings of the International Conference on Mössbauer Effect Applications*, Jaipur, India, 1981; Indian National Science Academy, New Delhi, 1982.

10 S. E. Wohler, R. J. Wittebort, S. M. Oh, D. N. Hendrickson, D. Inniss and C. E. Strouse, *J. Am. Chem. Soc.*, 1987, **109**, 2938; S. M. Oh, S. R. Wilson, D. N. Hendrickson, S. E. Wohler, R. J. Wittebort, D. Inniss and C. E. Strouse, *J. Am. Chem. Soc.*, 1987, **109**, 1073.

11 N. N. Greenwood and T. C. Gibb, *Mössbauer Spectroscopy*, Chapman and Hall, London, 1971.

12 K. Boukheddaden, J. Linares, H. Rabah, A. Bousseksou, J. Nasser and F. Varret, *Chem. Phys.*, 1993, **110**, 47; K. Boukheddaden, J. Linares, S. Galam, A. Bousseksou, J. Nasser and F. Varret, *J. Mol. Cryst. Liq. Cryst.*, 1993, **234**, 263.

13 S. M. Oh, D. N. Hendrickson, K. L. Hassett and R. E. Davis, *J. Am. Chem. Soc.*, 1985, **107**, 8009.

14 C. P. Slichter and H. G. Drickamer, *J. Chem. Phys.*, 1972, **56**, 2142; K. F. Purcell and M. P. Edward, *Inorg. Chem.*, 1984, **23**, 2620; J. Wajnflasz, *J. Phys.*, 1970, **C40**, 537; R. A. Bari and J. Sivardière, *J. Phys. Rev. B*, 1972, **5**, 4466; H. Spiering, E. Meissner, H. Köppen, E. W. Müller and P. Gütlich, *Chem. Phys.*, 1982, **68**, 65; A. Bousseksou, H. Constant and F. Varret, *J. Phys. I*, 1995, **5**, 747.

15 S. Nakashima, A. Nishimori, Y. Masuda, H. Sano and M. Sorai, *J. Phys. Chem. Solids*, 1991, **52**, 1169.

16 C. Stadler, J. Daub, J. Köhler, R. W. Saalfrank, V. Coropceanu, V. Schünemann, C. Ober, A. X. Trautwein, St. F. Parker, M. Poyraz, T. Inomata and R. D. Cannon, *J. Chem. Soc., Dalton Trans.*, 2001, 3373; R. D. Cannon, U. A. Jayasooriya, R. P. White and S. K. Arap Koske, *Spectrochim. Acta, Part A*, 1993, **49**, 1787.

17 M. N. Burnett and C. K. Johnson, ORTEP3, Report ORNL-6895, Oak Ridge National Laboratory, Oak Ridge, TN, 1996.